

Electrochemically Mediated Syntheses of Titanium(III)-Based Metal–Organic Frameworks

Alexandra M. Antonio, Joel Rosenthal,*¹ and Eric D. Bloch*²

Department of Chemistry and Biochemistry, University of Delaware, Newark, Delaware 19716, United States

Supporting Information

ABSTRACT: Although metal–organic frameworks featuring coordinatively unsaturated transition metal sites are relatively common, examples with redox-active cations are rare. In this report, we describe the electrochemically mediated synthesis of Ti^{III} -MIL-101 from the inexpensive Ti^{4+} precursor TiCl_4 . The framework obtained via electrosynthesis is identical to that prepared from the significantly more expensive and air-sensitive starting material TiCl_3 . The above electrosynthetic strategy was also extended to prepare Ti^{III} -MIL-100 and two high-quality extended Ti^{III} -MIL structures, for the first time. These materials represent examples of titanium-based MOFs with extended pore structures. Several physical methods demonstrate that these materials are superior in quality to samples of the analogous MOFs prepared via conventional routes from starting exogenous TiCl_3 . Given the ease with which the electrosyntheses may be carried out and their compatibility with a broad range of bridging ligands, we expect that this new methodology will find utility for the synthesis of a number of novel materials containing coordinatively unsaturated, redox-active metal cations.

Metal–organic frameworks (MOFs) have garnered considerable attention as they display high surface areas,^{1–3} tunable pore chemistry,^{4–6} and can be prepared from virtually any transition metal cation. These factors distinguish MOFs as highly tunable for numerous applications.⁷ Of the broad material space that is occupied by MOFs, those featuring accessible metal cations on their pore surface are particularly interesting as such systems can facilitate selective gas binding,⁸ high-density gas storage,⁹ sensing,¹⁰ and serve as sites for small-molecule activation and catalysis.¹¹ However, particularly for the latter which require redox-active metal cation sites, the number of reported materials is limited.^{12–16} For example, although numerous Cr^{3+} MOFs exist, there are few examples containing this metal in the 2+ oxidation state.¹⁷ Similarly, many examples of Ti^{4+} metal–organic frameworks have been reported,^{18–21} but to date there is a single Ti^{3+} -based MOF.²² This material, Ti^{III} -MIL-101 (Figure 1), is based on trimeric clusters connected to terephthalic acid (H_2bdc) and features a high BET surface area, exposed Ti^{3+} sites, and strong $\text{Ti}-\text{O}_2$ interactions via the formation of peroxide adducts. Further, its exposed Ti^{3+} sites are substrate accessible and can strongly bind gas molecules such as CO_2 and H_2 .

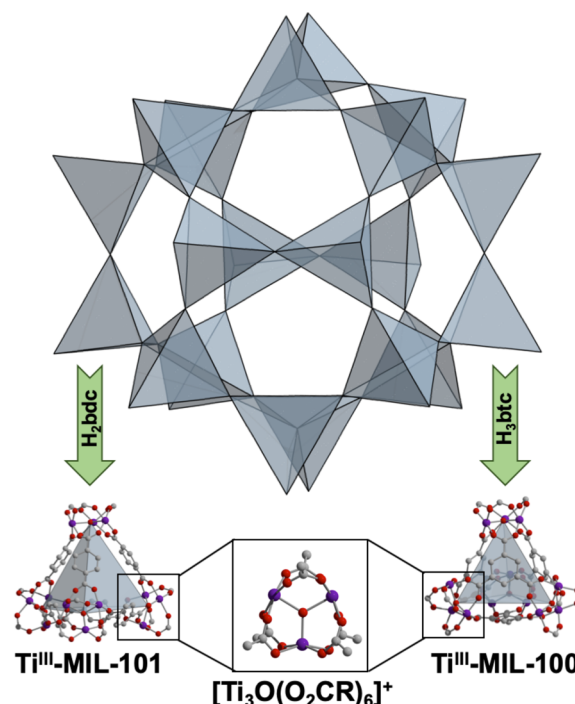


Figure 1. Portions of the MIL-100 and MIL-101 structure types that depict the large pores in the materials. Use of a linear dicarboxylate such as H_2bdc generates the MIL-101 structure; use of a triangular tricarboxylate such as H_3btc generates the MIL-100 structure.

The preparation of MOFs that are redox active and/or based upon metals in nontraditional or difficult to access oxidation states generally relies on the use of air-sensitive starting materials, necessitating the use of rigorously air-free reaction conditions and limiting materials discovery throughput. Moreover, for many metal ions in reduced oxidation states, the number of available starting materials is limited, as the synthesis of a metal–organic framework often relies on screening a number of parameters, including counteranion identity, placing additional bottlenecks on discovery of new structures.²³ In addressing these limitations, electrochemical methods present an intriguing alternative strategy for synthesis of reduced MOF materials.

Redox reactivity has been coupled to synthesis of MOFs. For example, redox chemistry has been used to drive ligand deprotonation reactions coupled to MOF syntheses.²⁴ Addi-

Received: May 10, 2019

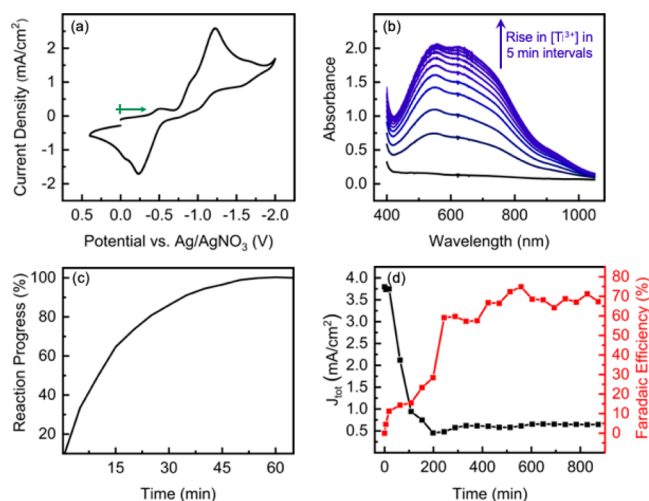


Figure 2. (a) Cyclic voltammogram recorded of TiCl_4 (1.0 mM) in 10:1 DMF:EtOH containing 0.1 M TBAPF₆ at a scan rate of 100 mV/s. (b) UV-vis absorption spectra of a $\text{TiCl}_4/\text{H}_2\text{bdc}$ DMF:EtOH solution containing 0.1 M TBAPF₆ during CPE at $E_{\text{applied}} = -1.20$ V. (c) Change in absorbance at $\lambda = 650$ nm during CPE described in (b). (d) Total current density and overall Faradaic efficiency for TiCl_4 and H^+ reduction from $\text{TiCl}_4/\text{H}_2\text{bdc}$ DMF:EtOH solution ($E_{\text{applied}} = -1.20$ V).

tionally, electrochemical dissolution of metallic anodes to generate oxidized metal ions (i.e., $\text{M}^0 \rightarrow \text{M}^{n+}$), has been utilized to synthesize Cu^{2+} and Zn^{2+} based MOFs.^{25–28} Despite these examples, we are aware of no published examples in which electrochemistry has been leveraged to alter the oxidation state of a dissolved metal ion in solution prior to MOF synthesis. Such a strategy is attractive as it can allow for the oxidation state of dissolved ions to be rapidly tuned via controlled potential electrolysis (CPE) for the targeted synthesis of MOFs containing metal centers in nontraditional, reduced oxidation states. Additionally, this strategy permits the large number of high oxidation state metal starting materials that are inexpensive and readily accessible to be converted to higher value reduced forms and facilitate the discovery of new materials containing metal ions in reactive oxidation states. This method also has the advantage that a larger number of reaction conditions can be screened, as they can be set up in the presence of air and then deoxygenated prior to electrochemical reduction. To this end, we targeted the synthesis of novel Ti^{3+} frameworks given their scarcity and potential for small molecule storage and activation.

The Ti^{3+} based MOF $\text{Ti}^{\text{III}}\text{-MIL-101}$ can be prepared by reaction of exogenous TiCl_3 with terephthalic acid (H_2bdc) at 120 °C in 10:1 *N,N*-dimethylformamide (DMF):ethanol for 18 h under rigorously air-free conditions. In order to prepare this material from Ti^{3+} generated electrochemically from Ti^{4+} sources, we utilized cyclic voltammetry (CV) to determine potentials (Figures S1–S3) at which Ti^{3+} can be generated from a series of Ti^{4+} based sources (e.g., TiCl_4 , $\text{Ti}(\text{O}^i\text{Pr})_4$, Cp_2TiCl_2). In particular, CVs recorded for solutions of TiCl_4 (Figure 2a) showed a cathodic wave corresponding to Ti^{4+} reduction at $E_{\text{cat}} = -1.20$ V (all potentials reported versus Ag/AgNO₃). Preparative scale reduction of TiCl_4 by CPE at $E_{\text{applied}} = -1.20$ V using a nickel electrode could be monitored by UV-vis spectroscopy (Figure 2b,c). The complete reduction of starting Ti^{4+} to Ti^{3+} was accomplished in as little as 60 min. A 4 h CPE ($E_{\text{applied}} = -1.20$ V) of TiCl_4 in the presence H_2bdc

and 0.1 M TBAPF₆ as supporting electrolyte in a 10:1 DMF/EtOH mixture using a nickel foam working electrode, followed by heating at 120 °C for 18 h afforded a crystalline dark purple powder in high yield.

Powder X-ray diffraction experiments indicated the resulting material is isostructural to the previously reported $\text{Ti}^{\text{III}}\text{-MIL-101}$ phase (Figure S6). The structure is comprised of trimeric Ti^{3+} clusters connected to form tetrahedral building units with bdc^{2-} anions on their vertices. The tetrahedral units are edge linked to afford a structure containing two large mesoporous cages, one with both pentagonal and hexagonal windows and the other comprised solely of pentagonal windows. $\text{Ti}^{\text{III}}\text{-MIL-101}$ obtained via the previously reported solvothermal method from starting Ti^{3+} displays a BET (Langmuir) surface area of 2970 (4440) m^2/g .²² The corresponding material synthesized via electrochemical generation of Ti^{3+} from TiCl_4 has a BET (Langmuir) surface area of 3285 (4360) m^2/g . Although PXRD, SEM, XPS, and TGA analyses indicate the solvothermally and electrochemically generated materials are virtually indistinguishable, synthesis of the latter is accomplished using inexpensive TiCl_4 , as opposed to relying on exogenously prepared and highly air-sensitive TiCl_3 . Of further note is the fact that commercial TiCl_4 is routinely available in 99.9% (and higher) purity, while TiCl_3 is typically prepared via aluminum reduction that result in Ti^{3+} starting materials containing appreciable levels of Al^{3+} .

A particular advantage of electrochemically synthesized reduced metal frameworks is the management of proton balance throughout the reaction. Significant concentrations of H^+ are generated during the course of solvothermal MOF syntheses as ligands are deprotonated to form M-L bonds. As many MOF syntheses are dependent on pH, the continually increasing proton concentration can complicate synthesis of phase-pure materials. The electrosynthetic strategy described above provides a convenient means to manage H^+ build up associated with formation of the bdc^{2-} anions needed for $\text{Ti}^{\text{III}}\text{-MIL-101}$ synthesis. The nickel foam working electrodes used to generate the Ti^{3+} from TiCl_4 show excellent HER activity at significantly lower potentials than those used for the reduction of Ti^{4+} .²⁹ Accordingly, CPE of the $\text{TiCl}_4/\text{H}_2\text{bdc}$ solutions with the nickel cathode not only generates Ti^{3+} , but also reduces the carboxylic acid protons to generate the bdc^{2-} ligands and H_2 , which is evolved from the cathode compartment.

To follow the production of H_2 over the course of the CPE, we monitored the reaction headspace during $\text{Ti}^{\text{III}}\text{-MIL-101}$ electrosynthesis via gas chromatography.^{30,31} Initial formation of H_2 was detected within as little as 5 min and plateaued after ~3–5 h. Initial Faradaic efficiencies for HER were <20% and slowly increased to ~70% as concentrations of Ti^{4+} were depleted to generate Ti^{3+} . In accounting for both the reduction of TiCl_4 to Ti^{3+} and H_2bdc (or H_3btc , vide infra) protons to H_2 , we consistently observed net current efficiencies in excess of 75% over the course of the entire CPE.

Given the potentially broad applicability of MOF electrosynthesis from soluble metal precursors, we sought to employ this method to expand the library of Ti^{3+} MOFs by targeting other multitopic carboxylate-based ligands. Since the $\mu_3\text{-O}$ centered trimeric cluster is ubiquitous to a large number of MIL-type MOFs, we targeted H_3btc -based MIL-100. This structure has previously been reported for trivalent Al,³² Sc,³³ V,³⁴ Cr,³⁵ Fe,³⁶ and mixed-metal systems and features connectivity that is analogous to the MIL-101 structure type, but where ligands occupy sites on the faces rather than vertices

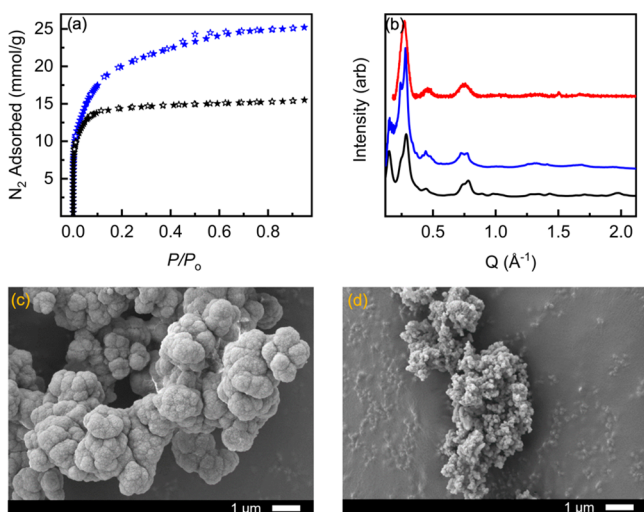


Figure 3. (a) N_2 adsorption in Ti^{III} -MIL-100 at 77 K of electrochemically (blue) and solvothermally synthesized (black) materials. (b) PXRD patterns of electrochemically (blue) and solvothermally synthesized (red) Ti^{III} -MIL-100 as compared to the predicted powder pattern (black). SEM images for (c) electrochemically and (d) solvothermally synthesized Ti^{III} -MIL-100.

of the tetrahedral building units. The electrochemical reduction of a $TiCl_4/H_3btc$ DMF:EtOH (10:1) solution containing 0.1 M TBAPF₆ followed by reaction at 120 °C for 18 h afforded the target material, as confirmed by powder X-ray diffraction (Figure 3). Interestingly, identical solvothermal reaction conditions utilizing commercial $TiCl_3$ rather than electrochemically reduced $TiCl_4$ afforded MOF powders with significantly lower uniformity (Figure 3). After thorough solvent exchanges and activation at 100 °C the solvothermally and electrochemically prepared materials showed BET (Langmuir) surface areas of 1304 (1568) and 1736 (2708) m^2/g , respectively (Figure 3a). The latter value is in good agreement with those reported for analogous MIL-100 materials.^{33,35}

Despite several attempts, solvothermal syntheses utilizing exogenous $TiCl_3$ as starting material consistently afforded frameworks with lower surface areas compared to those obtained using Ti^{3+} that had been electrochemically generated from $TiCl_4$. The lower surface areas obtained for the solvothermal materials may coincide with a Ti^{4+} -based framework with MIL-100 topology exhibiting a BET surface area of 1321 m^2/g that was recently reported.³⁷ We note that XPS analysis of solvothermally prepared samples of both Ti^{III} -MIL-101 and Ti^{III} -MIL-100 show that each retain chloride as a charge-balancing anion in the frameworks. Electrochemically prepared samples of these two Ti^{3+} -based frameworks both contain fluoride anions (in place of chloride), which is presumed to originate from the TBAPF₆ supporting electrolyte.

To determine whether the presence of supporting electrolyte improved the surface area of the electrochemically prepared Ti^{III} -MIL-100, TBAPF₆ was added to the solvothermal reaction mixture (exogenous $TiCl_3/H_3btc$). The thusly obtained dark brown product was both amorphous and nonporous. Further, solvothermal syntheses with exogenous $TiCl_3/H_3btc$ consistently afforded materials of smaller particle size (Figure 3d) as compared to syntheses utilizing electrochemically reduced $TiCl_4$ (Figure 3c).

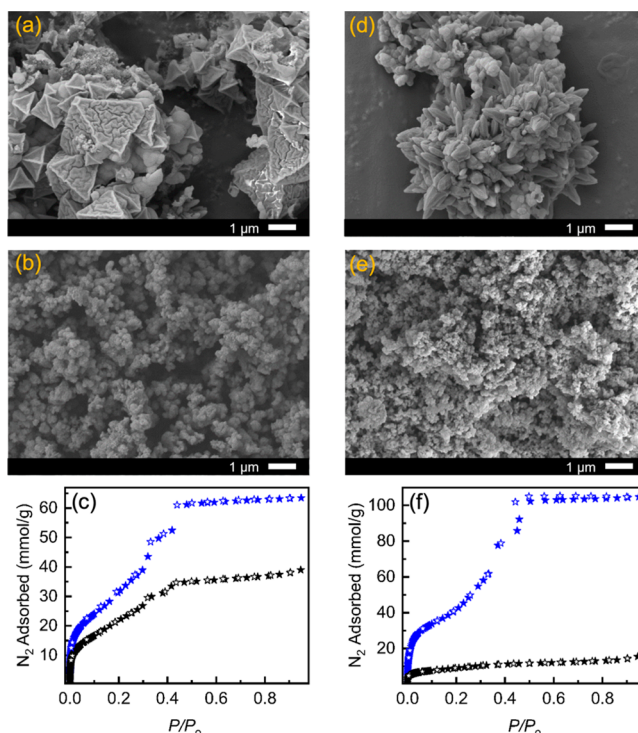


Figure 4. SEM images for (a) electrochemically and (b) solvothermally synthesized Ti^{III} -MIL-101-bpdc. (c) N_2 adsorption in Ti^{III} -MIL-101-bpdc at 77 K. SEM images for (d) electrochemically and (e) solvothermally synthesized Ti^{III} -MIL-100-tatb. (f) N_2 adsorption in Ti^{III} -MIL-100-tatb at 77 K. (Blue data = electrochemically prepared samples from $TiCl_4$; black data = solvothermally prepared samples from exogenous $TiCl_3$).

Given the near complete dearth of Ti^{3+} -based metal–organic frameworks, we sought to further expand the scope of this method to extended pore structures. Although materials of this type based on the M_3O building block have been reported, they typically feature surface areas that are significantly lower than values that are calculated for pristine structures. MIL-101(Fe)_BPDC, which is a biphenyldicarboxylate-based material that adopts the MIL-101 structure type, displays a BET surface area of just 210 m^2/g as compared to the theoretical value of 4500 m^2/g .³⁸ A MIL-100 structure based on an expanded tritopic (H_3btb) linker displays a BET surface area of just 26 m^2/g versus the expected value of 3990 m^2/g .³⁸

By adopting the straightforward electrosynthetic strategy developed for Ti^{III} -MIL-101 and Ti^{III} -MIL-100 (vide supra), we have been able to isolate high-quality extended pore Ti^{3+} based MOFs for the first time. Electrochemical reduction of a $TiCl_4$ solution containing either 4,4'-biphenyldicarboxylic acid (H_2bpdc) or 4,4',4''-[1,3,5]triazine-2,4,6-triyl-tris-benzoic acid (H_3tatb) followed by heating at 120 °C for 18 h afforded Ti^{III} -MIL-101-bpdc and Ti^{III} -MIL-100-tatb, respectively. Ti^{III} -MIL-101-bpdc displays a BET surface area of 3263 m^2/g and a pore volume of 2.20 cm^3/g . As shown in Table S2, these values are ~50% higher than those realized for samples of Ti^{III} -MIL-101-bpdc prepared solvothermally from exogenous $TiCl_3$ and H_2bpdc (2139 m^2/g and 1.32 cm^3/g). Similarly, electrochemically synthesized Ti^{III} -MIL-100-tatb displays a BET surface area and pore volume of 5842 m^2/g and 4.04 cm^3/g (Figure 4). These values dwarf those realized for analogous solvothermally prepared samples (740 m^2/g and 0.49 cm^3/g). The pore volume of the electrosynthesized Ti^{III} -MIL-100-

tatb (note: this structure is also referred to as PCN-333)²¹ is in excellent agreement with the value reported for the analogous Al-based MOF, PCN-333 (3.81 cm³/g).³⁹ The electrochemically synthesized materials also feature larger and more well-defined particle sizes (Figure 4) and increased crystallinities (Figures S10, S11).

In conclusion, we have leveraged electrochemical methods to synthesize reduced metal–organic frameworks. Electrochemical synthesis of Ti^{III}-MIL-101, Ti^{III}-MIL-100, Ti^{III}-MIL-101-bpdc, and Ti^{III}-MIL-100-tatb using the inexpensive, accessible, and highly pure Ti⁴⁺-based starting material, TiCl₄, generated frameworks with crystallinities and adsorption properties that are as good or superior to those of materials synthesized using exogenous/commercial TiCl₃. The electrochemically mediated synthetic strategy we have developed has provided the first reported route to Ti^{III}-MIL-100 and to high-quality samples of Ti³⁺-based MOFs with extended pore structures and surface areas that approach 6000 m²/g.

The electrosynthetic methods disclosed in this report not only generate the high-purity Ti³⁺ ions from which Ti^{III}-MIL-101 and Ti^{III}-MIL-100 structure types are built, but also provide a means to manage solution pH, as the H⁺ ions generated upon formation of the frameworks' Ti³⁺–O₂C–Ar bonds are readily reduced and evolved as H₂ gas. Accordingly, the methods outlined herein provide a new strategy for the electrochemically mediated synthesis of new redox-active metal–organic frameworks and for the isolation of reduced MOF materials.

■ ASSOCIATED CONTENT

● Supporting Information

The Supporting Information is available free of charge on the ACS Publications website at DOI: 10.1021/jacs.9b05035.

Detailed experimental procedures; Spectroscopic and PXRD data (PDF)

■ AUTHOR INFORMATION

Corresponding Authors

*E-mail: joelr@udel.edu.

*E-mail: edb@udel.edu.

ORCID

Joel Rosenthal: 0000-0002-6814-6503

Eric D. Bloch: 0000-0003-4507-6247

Notes

The authors declare no competing financial interest.

■ ACKNOWLEDGMENTS

We thank Benjamin Trump for help with powder X-ray diffraction experiments. This work was supported by a University of Delaware Research Foundation-Strategic Initiatives Grant to E.D.B. and J.R. E.D.B. also thanks the University of Delaware for startup funds that made this work possible. This research used resources of the Advanced Photon Source, a U.S. Department of Energy (DOE) Office of Science User Facility operated for the DOE Office of Science by Argonne National Laboratory under Contract No. DE-AC02-06CH11357. We thank the staff of 17-BM for help with synchrotron X-ray data collection. A portion of this work was supported by the National Institutes of Health under award number P20GM104316. Faradaic efficiencies were determined using instrumentation obtained through NSF CHE1352120.

■ REFERENCES

- (1) Honicke, I. M.; Senkovska, I.; Bon, V.; Baburin, I. A.; Bonisch, N.; Raschke, S.; Evans, J. D.; Kaskel, S. Balancing Mechanical Stability and Ultrahigh Porosity in Crystalline Framework Materials. *Angew. Chem., Int. Ed.* **2018**, *57*, 13780–13783.
- (2) Farha, O. K.; Eryazici, I.; Jeong, N. C.; Hauser, B. G.; Wilmer, C. E.; Sarjeant, A. A.; Snurr, R. Q.; Nguyen, S. T.; Yazaydin, A. O.; Hupp, J. T. Metal-Organic Framework Materials with Ultrahigh Surface Areas: Is the Sky the Limit? *J. Am. Chem. Soc.* **2012**, *134*, 15016–15021.
- (3) Furukawa, H.; Ko, N.; Go, Y. B.; Aratani, N.; Choi, S. B.; Choi, E.; Yazaydin, O.; Snurr, R. Q.; O'Keefe, M.; Kim, J.; Yaghi, O. M. Ultrahigh Porosity in Metal-Organic Frameworks. *Science* **2010**, *329*, 424–428.
- (4) Nguyen, J. G.; Cohen, S. M. Moisture-Resistant and Superhydrophobic Metal-Organic Frameworks Obtained via Postsynthetic Modification. *J. Am. Chem. Soc.* **2010**, *132*, 4560–4561.
- (5) Zhao, D.; Timmons, D. J.; Yuan, D.; Zhou, H.-C. Tuning the Topology and Functionality of Metal-Organic Frameworks by Ligand Design. *Acc. Chem. Res.* **2011**, *44*, 123–133.
- (6) Yaghi, O. M.; O'Keefe, M.; Ockwig, N. W.; Chae, H. K.; Eddaoudi, M.; Kim, J. Reticular Synthesis and the design of new materials. *Nature* **2003**, *423*, 705–714.
- (7) Furukawa, H.; Cordova, K. E.; O'Keefe, M.; Yaghi, O. M. The Chemistry and Applications of Metal-Organic Frameworks. *Science* **2013**, *341*, 1230444.
- (8) Li, J.-R.; Sculley, J.; Zhou, H.-C. Metal-Organic Frameworks for Separations. *Chem. Rev.* **2012**, *112*, 869–932.
- (9) Morris, R. E.; Wheatley, P. S. Gas Storage in Nanoporous Materials. *Angew. Chem., Int. Ed.* **2008**, *47*, 4966–4981.
- (10) Sun, Y.-F.; Liu, S.-B.; Meng, F.-L.; Liu, J.-Y.; Jin, Z.; Kong, L.-T.; Liu, J.-H. Metal Oxide Nanostructures and Their Gas Sensing Properties: A Review. *Sensors* **2012**, *12*, 2610–2631.
- (11) Chen, B.; Xiang, S.; Qian, G. Metal-Organic Frameworks with Functional Pores for Recognition of Small Molecules. *Acc. Chem. Res.* **2010**, *43*, 1115–1124.
- (12) Bloch, E. D.; Murray, L. J.; Queen, W. L.; Chavan, S.; Maximoff, S. N.; Bigi, J. P.; Krishna, R.; Peterson, V. K.; Grandjean, F.; Long, G. J.; Smit, B.; Bordiga, S.; Brown, C. M.; Long, J. R. Selective Binding of O₂ over N₂ in a Redox-Active Metal-Organic Framework with Open Iron(II) Coordination Sites. *J. Am. Chem. Soc.* **2011**, *133*, 14814–14822.
- (13) Bloch, E. D.; Queen, W. L.; Hudson, M. R.; Mason, J. A.; Xiao, D. J.; Murray, L. J.; Flacau, R.; Brown, C. M.; Long, J. R. Hydrogen Storage and Selective, Reversible O₂ Adsorption in a Metal-Organic Framework with Open Chromium(II) Sites. *Angew. Chem., Int. Ed.* **2016**, *55*, 8605–8609.
- (14) Murray, L. J.; Dinca, M.; Yano, J.; Chavan, S.; Bordiga, S.; Brown, C. M.; Long, J. R. Highly Selective and Reversible O₂ Binding in Cr₃(1,3,5-benzenetricarboxylate)₂. *J. Am. Chem. Soc.* **2010**, *132*, 7856–7857.
- (15) Wade, C. R.; Dinca, M. Investigation of the synthesis, activation, and isosteric heats of CO₂ adsorption of the isostructural series of metal–organic frameworks M₃(BTC)₂ (M = Cr, Fe, Ni, Cu, Mo, Ru). *Dalton Trans* **2012**, *41*, 7931–7938.
- (16) Tulchinsky, Y.; Hendon, C. H.; Lomachenko, K. A.; Borfecchia, E.; Melot, B. C.; Hudson, M. R.; Tarver, J. D.; Korzynski, M. D.; Stubbs, A. W.; Kagan, J. J.; Lamberti, C.; Brown, C. M.; Dinca, M. Reversible Capture and Release of Cl₂ and Br₂ with a Redox-Active Metal-Organic Framework. *J. Am. Chem. Soc.* **2017**, *139*, S992–S997.
- (17) Park, J.; Perry, Z.; Chen, Y.-P.; Bae, J.; Zhou, H.-C. Chromium(II) Metal-Organic Polyhedra as Highly Porous Materials. *ACS Appl. Mater. Interfaces* **2017**, *9*, 28064–28068.
- (18) Dan-Hardi, M.; Serre, C.; Frot, T.; Rozes, L.; Maurin, G.; Sanchez, C.; Ferey, G. A New Photoactive Crystalline Highly Porous Titanium(IV) Dicarboxylate. *J. Am. Chem. Soc.* **2009**, *131*, 10857–10859.

- (19) Gao, J.; Miao, J.; Li, P.-Z.; Teng, W. Y.; Yang, L.; Zhao, Y.; Liu, B.; Zhang, Q. A p-type Ti(IV)-based metal-organic framework with visible-light photo-response. *Chem. Commun.* **2014**, *50*, 3786–3788.
- (20) Yuan, S.; Liu, T.-F.; Feng, D.; Tian, J.; Wang, K.; Qin, J.; Zhang, Q.; Chen, Y.-P.; Bosch, M.; Zou, L.; Teat, S. J.; Dalgarno, S. J.; Zhou, H.-C. A single crystalline porphyrinic titanium metal-organic framework. *Chem. Sci.* **2015**, *6*, 3926–3930.
- (21) Zou, L.; Feng, D.; Liu, T.-F.; Chen, Y.-P.; Yuan, S.; Wang, K.; Wang, X.; Fordham, S.; Zhou, H.-C. A Versatile Synthetic Route for the Preparation of Titanium Metal–Organic Frameworks. *Chem. Sci.* **2016**, *7* (2), 1063–1069.
- (22) Mason, J. A.; Darago, L. E.; Lukens, W. W.; Long, J. R. Synthesis and O₂ Reactivity of a Titanium(III) Metal–Organic Framework. *Inorg. Chem.* **2015**, *54*, 10096–10104.
- (23) Maniam, P.; Stock, N. Investigation of Porous Ni-Based Metal–Organic Frameworks Containing Paddlewheel-Type Inorganic Building Units via High-Throughput Methods. *Inorg. Chem.* **2011**, *50*, 5085–5097.
- (24) Li, M.; Dinca, M. Reductive Electrosynthesis of Crystalline Metal–Organic Frameworks. *J. Am. Chem. Soc.* **2011**, *133*, 12926–12929.
- (25) Li, W.-J.; Lü, J.; Gao, S.-Y.; Li, Q.-H.; Cao, R. Electrochemical preparation of metal–organic framework films for fast detection of nitro explosives. *J. Mater. Chem. A* **2014**, *2*, 19473–19478.
- (26) Martinez-Joaristi, A.; Juan-Alcañiz, J.; Serra-Crespo, P.; Kapteijn, F.; Gascon, J. Electrochemical Synthesis of Some Archetypical Zn²⁺, Cu²⁺, and Al³⁺ Metal Organic Frameworks. *Cryst. Growth Des.* **2012**, *12*, 3489–3498.
- (27) Ameloot, R.; Stappers, L.; Franssaer, J.; Alaerts, L.; Sels, B. F.; De Vos, D. E. Patterned Growth of Metal–Organic Framework Coatings by Electrochemical Synthesis. *Chem. Mater.* **2009**, *21*, 2580–2582.
- (28) Rubio-Martinez, M.; Avci-Camur, C.; Thornton, A. W.; Imaz, I.; MasPOCH, D.; Hill, M. R. New Synthetic routes towards MOF production at scale. *Chem. Soc. Rev.* **2017**, *46*, 3453–3480.
- (29) Thoi, V. S.; Sun, Y.; Long, J. R.; Chang, C. J. Complexes of earth-abundant metals for catalytic electrochemical hydrogen generation under aqueous conditions. *Chem. Soc. Rev.* **2013**, *42*, 2388–2400.
- (30) DiMeglio, J. L.; Rosenthal, J. Selective Conversion of Carbon Dioxide to CO with High Efficiency using an Inexpensive Bismuth Based Electrocatalyst. *J. Am. Chem. Soc.* **2013**, *135*, 8798–8801.
- (31) Atifi, A.; Boyce, D. W.; DiMeglio, J. L.; Rosenthal, J. Directing the Outcome of CO₂ Reduction at Bismuth Cathodes Using Varied Ionic Liquid Promoters. *ACS Catal.* **2018**, *8*, 2857–2863.
- (32) Volklinger, C.; Popov, D.; Loiseau, T.; Férey, G.; Burghammer, M.; Riekel, C.; Haouas, M.; Taulelle, F. Synthesis, Single-Crystal X-ray Microdiffraction, and NMR Characterizations of the Giant Pore Metal–Organic Framework Aluminum Trimesate MIL-100. *Chem. Mater.* **2009**, *21*, 5695–5697.
- (33) Mitchell, L.; Gonzalez-Santiago, B.; Mowat, J. P. S.; Gunn, M. E.; Williamson, P.; Acerbi, N.; Clarke, M. L.; Wright, P. A. Remarkable Lewis acid catalytic performance of the scandium trimesate metal organic framework MIL-100(Sc) for C–C and C = N bond-forming reactions. *Catal. Sci. Technol.* **2013**, *3*, 606–617.
- (34) Lieb, A.; Leclerc, H.; Devic, T.; Serre, C.; Margiolaki, I.; Mahjoubi, F.; Lee, J. S.; Vimont, A.; Daturi, M.; Chang, J.-S. MIL-100(V) – A mesoporous vanadium metal organic framework with accessible metal sites. *Microporous Mesoporous Mater.* **2012**, *157*, 18–23.
- (35) Llewellyn, P. L.; Bourrelly, S.; Serre, C.; Vimont, A.; Daturi, M.; Hamon, L.; De Weireld, G.; Chang, J. S.; Hong, D. Y.; Hwang, Y. K.; Jung, S. H.; Férey, G. High Uptakes of CO₂ and CH₄ in Mesoporous Metal–Organic Frameworks MIL-100 and MIL-101. *Langmuir* **2008**, *24*, 7245–7250.
- (36) Yoon, J. W.; Seo, Y.-K.; Hwang, Y. K.; Chang, J.-S.; Leclerc, H.; Wuttke, S.; Bazin, P.; Vimont, A.; Daturi, M.; Bloch, E.; Llewellyn, P. L.; Serre, C.; Horcajada, P.; Greneche, J.-M.; Rodrigues, A. E.; Férey, G. Controlled Reducibility of a Metal–Organic Framework with Coordinatively Unsaturated Sites for Preferential Gas Sorption. *Angew. Chem., Int. Ed.* **2010**, *49*, 5949–5952.
- (37) Castells-Gil, J.; Padial, N. M.; Almora-Barrios, N.; da Silva, I.; Mateo, D.; Albero, J.; Garcia, H.; Marti-Gastaldo, C. De novo synthesis of mesoporous photoactive titanium(IV)-organic frameworks with MIL-100 topology. *Chem. Sci.* **2019**, *10*, 4313–4321.
- (38) Horcajada, P.; Chevreau, H.; Heurtaux, D.; Benyettou, F.; Salles, F.; Devic, T.; Garcia-Marquez, A.; Yu, C.; Lavrard, H.; Dutson, C. L.; Magnier, E.; Maurin, G.; Elkalm, E.; Serre, C. Extended and functionalized porous iron(III) tri- or dicarboxylates with MIL-100/101 topologies. *Chem. Commun.* **2014**, *50*, 6872–6874.
- (39) Feng, D.; Liu, T.-F.; Su, J.; Bosch, M.; Wei, Z.; Wan, W.; Yuan, D.; Chen, Y.-P.; Wang, X.; Wang, K.; Lian, X.; Gu, Z.-Y.; Park, J.; Zou, X.; Zhou, H.-C. Stable metal-organic frameworks containing single-molecule traps for enzyme encapsulation. *Nat. Commun.* **2015**, *6*, 5979.